Solar Energy 223 (2021) 238–247

Contents lists available at ScienceDirect

Solar Energy

journal homepage: www.elsevier.com/locate/solener

Identifying snow in photovoltaic monitoring data for improved snow loss modeling and snow detection

Mari B. Øgaard [a,b,*], Bjørn L. Aarseth [a,b], Åsmund F. Skomedal [b], Heine N. Riise [b], Sabrina Sartori [a], Josefine H. Selj [a,b]

[a] Department of Technology Systems, University of Oslo, Gunnar Randers vei 19, 2007 Kjeller, Norway
[b] Solar Power Systems Department, Institute for Energy Technology, Instituttveien 18, 2007 Kjeller, Norway

ARTICLE INFO

Keywords:
Photovoltaic systems
Snow
Snow loss modeling
Snow detection
PV performance
Soiling

ABSTRACT

As cost reductions have made photovoltaics (PV) a favorable choice also in colder climates, the number of PV plants in regions with snowfalls is increasing rapidly. Snow coverage on the PV modules will lead to significant power losses, which must be estimated and accounted for in order to achieve accurate energy yield assessment and production forecasts. Additionally, detection and separation of snow loss from other system losses is necessary to establish robust operation and maintenance (O&M) routines and performance evaluations.

Snow loss models have been suggested in the literature, but developing general models is challenging, and validation of the models are lacking. Characterization and detection of snow events in PV data has not been widely discussed.

In this paper, we identify the signatures in PV data caused by different types of snow cover, evaluate and improve snow loss modeling, and develop snow detection. The analysis is based on five years of data from a commercial PV system in Norway. In an evaluation of four snow loss models, the Marion model yields the best results. We find that system design and snow depth influence the natural snow clearing, and by expanding the Marion model to take this into account, the error in the modeled absolute loss for the tested system is reduced from 23% to 3%. Based on the improved modeling and the identified data signatures we detect 97% of the snow losses in the dataset. Endogenous snow detection constitutes a cost-effective improvement to current monitoring systems.

1. Introduction

Due to a substantial decline in the price of photovoltaic (PV) installations in recent years, large scale PV plants are increasingly common in cold climates with wintertime snowfalls (Burnham et al., 2020; Hashemi et al., 2020; IEA, 2020; Jäger-Waldau, 2020). This development necessitates robust methods for analyzing PV yield and performance, as well as flexible monitoring and forecasting solutions in snowy conditions. Thus, accurate snow loss modeling and snow detection are required.

Snow losses are expected to vary significantly with climate, system configuration and from year to year. At its maximum, it might give monthly losses up to 100% in the winter season and annual losses above 30% (Pawluk et al., 2019). Consequently, it is an important parameter to consider in simulation and yield assessment of future PV systems in locations with snowfalls, as well as in production forecasts and performance and loss analysis of historical PV data. Snow losses will also introduce significant challenges in monitoring, giving signatures in the production data which resemble failures. A full snow cover gives an electrical response similar to an inverter breakdown. A partial snow cover leading to partial shading can give electrical losses (Schill et al., 2015) similar to serious PV module failures (Tsanakas et al., 2016). When using empirical or machine learning based methods for PV modeling, snow events in the training data will perturb the correlations between irradiance, temperature and production. These perturbations can increase the uncertainty of the models (Øgaard et al., 2020).

Recent research has demonstrated that uncertainty in yield estimations (Bosman and Darling, 2018; Marion et al., 2013; Ryberg and Freeman, 2017; Townsend and Powers, 2011) and forecasting (Lorenz et al., 2011) can be reduced if snow loss models are included. Despite this, snow loss models are often not implemented in PV simulation software. The System Advisor Model (SAM) has implemented the model

* Corresponding author at: Department of Technology Systems, University of Oslo, Gunnar Randers vei 19, 2007 Kjeller, Norway.
E-mail address: mari.ogaard@its.uio.no (M.B. Øgaard).

https://doi.org/10.1016/j.solener.2021.05.023
Received 13 January 2021; Received in revised form 4 May 2021; Accepted 7 May 2021
Available online 28 May 2021

suggested by Marion et al. (Marion et al., 2013; Ryberg and Freeman, 2017), but in other software, snow is either not considered (PVGIS, 2020) or estimated by constant soiling values (PVsyst, 2020; Solargis, 2016), typically not related to the climatic conditions.

In PV monitoring, if at all considered, detection of snow is a more common approach than snow loss modeling. In the literature, snow detection methods based on dedicated or external sensors like weight sensors, web cameras and satellite data have been proposed (Aarseth et al., 2018; Andrews et al., 2013; Wirth et al., 2010). Ambient temperature (Lorenz et al., 2007) and module temperature (Øgaard et al., 2018) have been suggested as measurements that can be used to identify snow-related losses in PV monitoring and failure diagnosis. Except for this, identifying and characterizing the effects of snow in PV monitoring data, a prerequisite to separate snow losses from failures and a method to cost effectively detect snow, is not widely discussed.

Accurate snow loss modeling and robust snow detection are challenging, because the parameters influencing the snow cover and resulting PV system loss are manifold. The influential parameters range from weather conditions (irradiance, temperature, wind, etc.), to installation and technology specific configurations (tilt, module technology, ground/roof mounted, etc.) and type of snow. This is challenging for both physical and empirical models due to the amount of required input data. Existing snow loss models, use weather data and technical system configuration to either estimate (i) snow coverage or (ii) the losses directly (Pawluk et al., 2019). Most of the suggested methods are based on empirical approaches, including both simple linear relationships (Pawluk et al., 2019) and machine learning (Bashir et al., 2020; Hashemi et al., 2020). Validation of the models on other PV systems is typically lacking (Ryberg and Freeman, 2017). While the uncertainty for monthly and annual losses often are low compared to the size of the loss, the uncertainty on daily and higher time resolutions is high (Andrews and Pearce, 2012; Marion et al., 2013).

In particular, it is the process of natural snow clearing that is difficult to model. The main mechanisms of natural snow clearing are melting and sliding, both effects typically connected to ambient temperatures larger than 0 ℃ (Pawluk et al., 2019), but sliding at −10 °C has also been observed (Becker et al., 2006). Friction and adhesion between the snow and the solar panels are parameters that contribute to the complexity of natural snow clearing, as both are expected to vary with type of snow (Andrews et al., 2013; Pawluk et al., 2019). While wet snow has lower friction, it is also more likely to freeze to the module (Andenæs et al., 2018; Ross, 1995). Natural snow clearing is thus dependent on how temperature evolves with time. Additionally, system configurations like tilt and elements obstructing the path of snow sliding (e.g. the module frame (Riley et al., 2019), or little empty space below the modules giving ground/roof interference (Heidari et al., 2015)) will impact natural snow clearing. Technical system aspects might also impact the heat transfer to the system and thus the snow melting. Increased melting can e.g. be caused by absorbed reflected irradiance on the rear side for a ground mounted bifacial system (Burnham et al., 2019), or by poor roof insulation for a roof mounted system.

Because different types of modules have different shading response, snow losses and the signatures in the electrical data will also depend on type of modules (thin film or crystalline silicon, full or half cells, monofacial or bifacial), and for the most typical crystalline silicon (c-Si) module with three bypass diodes: whether the modules are installed in portrait or landscape orientation. When the snow slides down the tilted module, it typically shades the lower part, as shown in Fig. 1. This gives shading orthogonal to the substring current for modules installed in portrait orientation, and parallel to the substring current for modules installed in landscape. In the first case, all the substrings in the modules are impacted, in the second case, the shaded area can be bypassed by the bypass diodes. This can lead to significantly higher snow-related losses for modules installed in portrait orientation than modules installed in landscape orientation under similar partial snow covers (Andenæs et al., 2018; Andrews et al., 2013; van Noord et al., 2017). On the other hand,

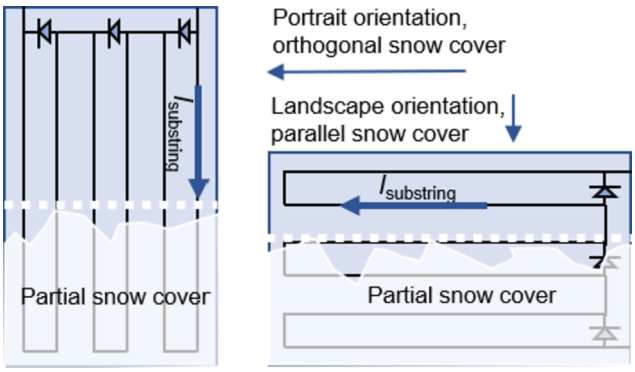

Fig. 1. Illustration of portrait and landscape module orientation and how a partial snow cover typically shades the tilted modules when it is sliding off the modules. A module installed in portrait is shaded orthogonal to the module substring current, and a module installed in landscape is shaded in parallel with the module substring current.

natural snow clearing has been observed to happen faster for modules in portrait orientation than for modules in landscape orientation (Burnham et al., 2020). One of the suggested explanations is that the frame impedes sliding more for modules in landscape. Additionally, if the modules are irradiated but generate no or low current (compared to the irradiance level), they are expected to be warmer because the energy is not converted to electricity (Teubner et al., 2019). Because modules in portrait will generate less current under partial snow cover, they will become warmer than modules in landscape, aiding the melting process.

The aim of this work is to (i) characterize the effect of snow in PV monitoring data, (ii) to assess and improve on existing PV snow loss models, and (iii) to develop snow detection methods for PV monitoring data. The main focus is on monofacial c-Si technology. To characterize the impact of different types of snow covers on the measured variables of a PV system, we have analyzed data from two PV systems in Norway with regular snow cover in the winter. The identified signatures in PV monitoring data caused by snow, are assessed by using simulations of shaded modules and transmittance measurements. The PV monitoring data is further used for evaluation and improvement of snow loss models, and both the improved snow loss models and the signatures are used in development of snow detection.

2. Methodology

2.1. PV monitoring data

The PV monitoring data utilized in this study is primarily from a commercial 185 kW_p roof top PV system. The data from the commercial system is complemented by detailed studies and experimental data obtained from a 4 kW_p ground mounted test system at the Institute for Energy Technology research facility. The commercial PV system is installed on a flat roof, the lowest part of the modules nearly touching the rooftop. The multicrystalline silicon PV modules are oriented East-West with a tilt of 10°, and installed in landscape orientation. This system configuration is typical for many of the larger PV systems in the Nordic countries. A tilt angle of 10° is not optimal for high latitude locations with respect to maximum production, but is typically used in installations on flat roof systems also at high latitudes to maximize roof coverage and to, in combination with the East-West orientation, achieve a more even production distribution through the year and the day. The test system has South-oriented crystalline silicon modules with a tilt of 28° installed in portrait orientation (FME Susoltech, 2020). The array height is two modules for the test system, and one module for the commercial system. Both systems are located approximately 60° North and 11° East.

For both systems, 5 years of data are collected. For the commercial

system, current, voltage and power data are collected from the inverters, and temperature and irradiance data are collected from the monitoring system of the installation. The data is logged at 5 min interval, and the DC inverter data are measured at maximum power point tracker level (MPPT). Three strings of 24 modules are connected in parallel to one MPPT. In the test system, the electrical data is measured at module level by power optimizers, and the recording interval of the data logging is 15 min. The effective in plane irradiance incident on the PV modules, i.e. the irradiance the modules can utilize (Stein and Farnung, 2017), is in both cases measured with a crystalline silicon reference cell in the plane of the PV modules. The measurement uncertainty of the irradiance is ± 5 W/m^2 $\pm$ 2.5% of reading. The module temperature is measured by a sensor attached to the rear side of the modules. Wind and humidity data was collected from nearby weather stations (Norsk Klimaservicesenter, 2020). To identify time periods with snow on the reference cells, the reference cell irradiance measurements are compared to measurements from irradiance sensors at the systems that are observed to be less effected by snow: a heated horizontal pyranometer at the commercial system, and a vertical pyranometer at the test system. To reduce the effect of snow-covered irradiance sensors on the analysis, the measurements from the heated horizontal pyranometer are used as a replacement of the in plane irradiance at the commercial system for days where the daily irradiation measured by the pyranometer irradiation is more than twice the daily reference cell irradiation.

At the test system, the transmittance of the snow cover on the modules was measured for different snow cover thicknesses, by measuring the irradiance on the front and rear side of a full size module glass with the same tilt as the PV modules, using a spectroradiometer (Spectral Evolution, PSR-1100F). The measurements were conducted over 7 days with different snow and irradiance conditions. Observations of the snow coverage on the modules were collected at the same time by sample images. Daily estimated snow data for the two locations, based on interpolated observational data are collected from seNorge.no (NVE, 2019).

2.2. Identification of snow signatures in PV monitoring data

2.2.1. Observed snow signatures

To study the signatures of snow in PV monitoring data, deviations compared to snow free production for electrical DC data (power, voltage, current) and module temperature in time periods after snow falls are evaluated. The evaluation is performed for both modules installed in landscape and portrait orientation.

The expected power, voltage and current for snow free conditions is modeled by a single diode model. Module datasheet values and PySAM (NREL, 2020) are used to estimate the diode ideality factor, light generated current, dark reverse saturation current, shunt resistance and series resistance at reference conditions, and the parameter for adjusting the short circuit current temperature coefficient, as described by Dobos (2012). These parameters together with the measured effective irradiance and cell temperature are used as inputs to the CEC model (Dobos, 2012), which estimates the photocurrent, saturation current, shunt resistance and thermal cell voltage. The expected electrical output for each module is estimated by solving the single diode equation based on the parameters estimated with the CEC model, as implemented in pvlib python (Holmgren et al., 2018). The constant system losses are estimated by comparing the modeled power to the measured power under snow free conditions. Based on this, some differences were observed in the angular response between the reference cell and the module strings, giving seasonal variation in the system losses. To compensate for this, the additional reflection loss of the modules, was modeled with the ASHRAE IAM model (Holmgren et al., 2018; Souka and Safwat, 1966) with an IAM adjustment parameter of 0.03. The expected PV module temperature is modeled by the cell temperature model from the Sandia Array Performance Model (SAPM) (Holmgren et al., 2018; King et al., 2004), where the module temperature is estimated based on global irradiance, ambient temperature, and wind speed.

Uncertainty in PV modeling is typically higher at lower irradiance and high angles of incidence, as it is challenging to capture all loss effects under these conditions. This can give a small absolute, but high relative, overestimation of the expected power and current in the wintertime, and thus overestimation of the snow losses in these parameters. Snow on the irradiance sensor can on the other hand lead to underestimation of both absolute and relative losses. On a monthly basis for the periods without snow, the mean absolute error in the daily modeled energy generation for the commercial system is up to 0.1 kWh/kW$_p$ in the summer months and down to 0.02 kWh/kW$_p$ in the winter months. For both systems, the mean absolute percentage error in daily modeled energy is 2% for most months, but in the darkest winter months when the energy generation can be <1 kWh/kW$_p$ per day, small deviations in the model can give high relative errors, up to 20%. When the expected energy generation is aggregated for longer time periods, the days with highest production and lowest uncertainty will dominate and reduce the relative uncertainty.

2.2.2. Simulated electrical snow signatures

The expected electrical signatures in PV module data for different snow covers are modeled using circuit simulations in MATLAB Simulink. A system with the same configuration as the commercial system described in Section 2.1 is modeled, with 60 cell modules having 3 bypass diodes each. A variable voltage source is used to trace the full IV curve of the modeled system. Solar cell blocks in Simulink are modeled by solving the single diode equation, and piecewise linear diodes are utilized as bypass diodes. The Simulink solar cell single diode parameters are fitted so that 60 cells in series match the IV characteristics of the commercial system. The simulations are performed for a case where the cell temperature is 25 °C and the irradiance is 450 W/m^2. Snow covers are simulated as a reduction in irradiance for the covered part of the modules, and the resulting power, current and voltage from the simulated IV trace are used to calculate electrical losses for different shading situations. The loss is calculated by comparing the yield of the snow-covered system with an unshaded, identical system. The covers are varied in size and transmittance, and the partial covers are modeled both for portrait and landscape module orientation, i.e. orthogonal and parallel to the substring current, respectively. The simulations are not validated through field data because we have no accurate measures of snow covers. This means we have no estimates of the performance of the simulation at low light conditions and what error is introduced by using the same cell temperature for all simulations, thereby not including the temperature differences caused by snow cover. The efficiency of the inverter at low irradiances, the MPPT voltage range of the inverter, and how the MPPT handles partial shading will also influence the loss in electrical parameters. We do, however, still believe that the simulations capture the general behavior at these conditions and help us understand how different snow covers impact electrical PV measurements.

2.3. Snow loss model evaluation

The calculated snow power loss, i.e. the deviation between the measured power and the modeled power (Section 2.2.1), is used to validate snow loss models. The data from the commercial system is used in the evaluation, as it has multiple identical arrays and is thus expected to give an insight into eventual loss variations for similar configurations. The tested models are the models suggested by Andrews and Pearce (2012), Powers et al. (2010), Townsend and Powers (2011), and Marion et al. (2013) as implemented in pvlib python (Holmgren et al., 2018; Ryberg and Freeman, 2017). The three first models aim to estimate the snow losses based on empirical correlations with different environmental parameters. Andrews and Pearce estimate daily losses based on a correlation between snow losses and irradiance, temperature, and the change in snow depth for the two last days. Powers et al. use a correlation between annual snow losses, snow depth and module tilt.

Townsend and Powers estimate monthly losses using a correlation between snow losses and humidity, temperature, irradiance, snow fall, and a ground interference parameter. The Marion model initially estimates the snow cover, and subsequently calculates the snow loss based on the snow cover estimate. The model assumes that when the snow starts to melt, it is cleared by sliding off the modules. Snowfall data are used to identify the presence of snow, and irradiance and module temperature are used to identify conditions where snow slides off the modules. Snow sliding is assumed to happen when:

$$T_{amb} > G_{POA}/m, \quad (1)$$

where T_{amb} is the ambient temperature, G_{POA} is the in plane irradiance and m is an empirically defined value of -80 W/(m^2 °C). How much the snow will slide, measured in fractions of the total row height, is determined by the tilt of the modules and an empirical sliding coefficient (sc):

$$Snow\ slide\ amount = sc^{*}\sin(tilt) \quad (2)$$

For roof mounted systems sc was found to be 0.20 (Holmgren et al., 2018; Marion et al., 2013). The snow loss is subsequently estimated from the calculated snow coverage and the number of parallel connected strings (including module substrings) along the row height, taking into account whether the modules are installed in portrait or landscape orientation (Holmgren et al., 2018). If a module substring is partially covered by snow, the capacity is assumed to be zero (Gilman et al., 2018). All snowfalls greater than 0 cm are included in the snow loss modeling.

3. Results and discussion

The impact of full and different levels of partial snow cover on the PV monitoring data is presented in Section 3.1.1. The results are assessed using simulations of shaded strings (Section 3.1.2) and transmittance measurements (Section 3.1.3). The signatures in the monitoring data caused by snow are summarized in Section 3.1.4. Evaluation and improvement of snow loss modeling is presented in Section 3.2. Based on the improved model and the snow signatures, a method for snow detection is proposed in Section 3.3.

3.1. Snow signatures

3.1.1. Observed snow signatures in PV monitoring data

Fig. 2 shows the daily losses in voltage, current and power for a time period with snow melting where the modules gradually are going from fully snow covered, through different levels of partial cover, to snow free. The event is in March/April, in a period with high irradiance, giving low relative uncertainty in the modeled expected value. The boxplot shows the variation in the measurements. In the beginning of the period, when the snow cover is assumed to be full and opaque, the losses in all electrical parameters are 100%. When the snow cover starts to melt, the first development is an increase in voltage. For some of the modules in the test system, voltage gain is registered. As the snow continues to melt, a stepwise reduction in voltage losses is observed, while the losses in current and power are gradually reduced. The variation in losses between different modules/inverters is large for partial snow cover, reflected in a large spread in the measured loss. For the test system (portrait orientation), where the loss is measured at module level and not aggregated for larger subarrays as for the commercial system, particularly large variations in both current and voltage are seen.

The module temperature is also significantly influenced by snow cover. Fig. 3 shows how the measured module temperatures in the test system develop compared to the ambient temperature and the modeled module temperature during the same melting period as in Fig. 2. The module temperature is quite stable at full snow cover with less pronounced diurnal variations than the ambient temperature. As the snow cover melts, the measured module temperatures are more impacted by irradiance and ambient temperature, and there are large variations between different module temperature sensors, due to the local variations

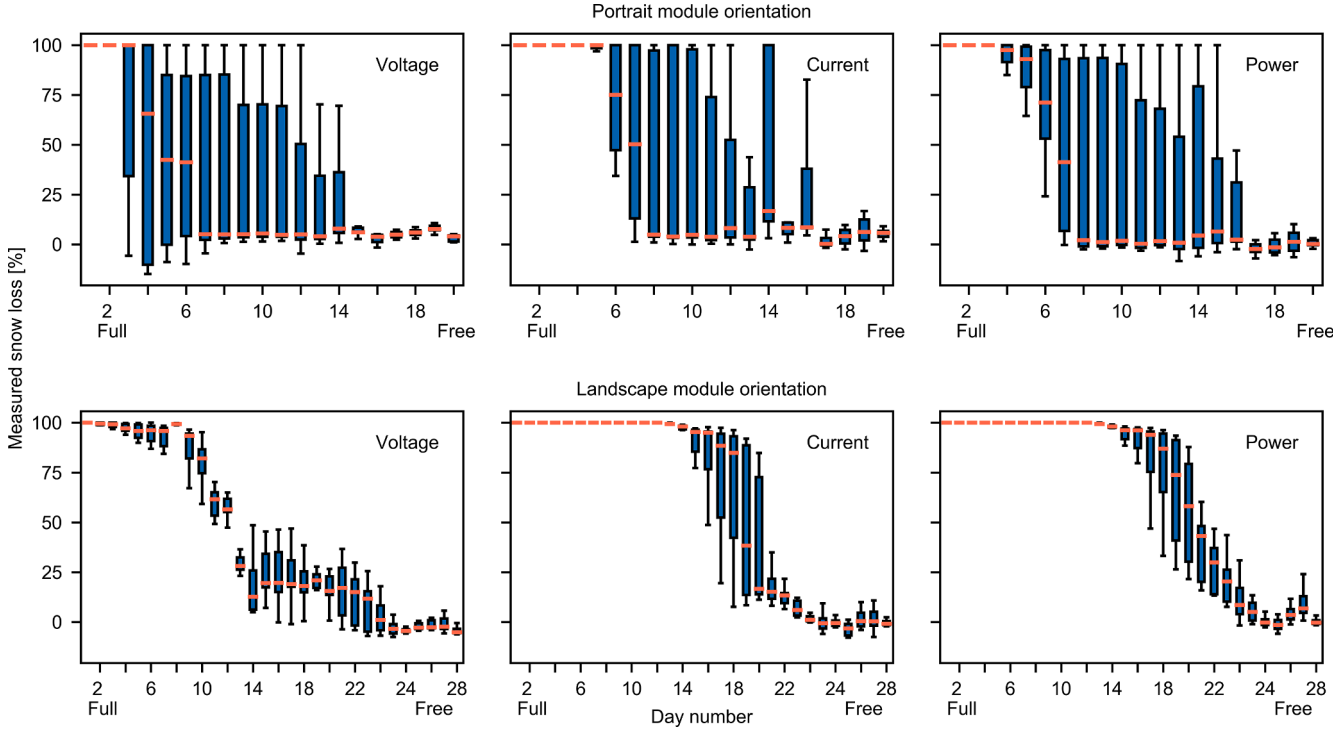

Fig. 2. The measured daily snow losses in voltage, current and power for the two different module orientations in a period where the modules go from fully covered, through different levels of partial cover, to snow free. The boxplot shows the variation in loss between different inverters/modules. The boxes extend from the first to the third quartile values of the data, with a line on the median. The whiskers extend to the maximum or minimum value within 1.5 times the interquartile range, and outliers are not included.

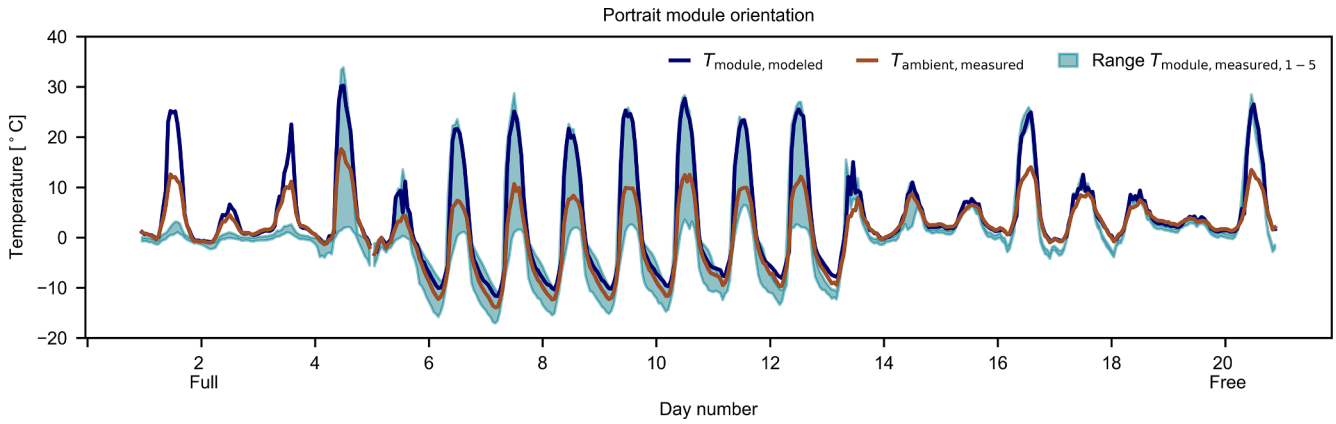

Fig. 3. Development of the modeled module temperature ($T_{module, modeled}$), the measured ambient temperature ($T_{ambient, measured}$), and the range of the measured module temperatures ($T_{mod, measured 1-5}$), in a snow melting period for the modules installed in portrait orientation.

in snow cover. The observed signatures illustrated in Figs. 2 and 3 are representative for the time periods after snow falls for the whole dataset. The electrical signatures for the days where exact snow coverage is measured through imaging, also support these observations.

3.1.2. Simulated electrical snow signatures

Fig. 4 shows the simulated losses in current, voltage and power as a function of snow coverage for modules installed in landscape and portrait orientation. The transmittance of the snow cover is 0 (opaque). As a function of snow coverage, the loss in current follows a simple relationship: If at least one cell in all module substrings is covered, the loss is 100%, and if there is at least one snow-free module substring, the loss is zero. The voltage loss is dependent on the snow free area (as seen for modules in portrait orientation with shading orthogonal to the substring current), but also on activation of bypass diodes (as seen for the modules in landscape orientation with shading in parallel with the substring current). As discussed in Section 2.2.2, we can expect additional electrical losses in the measured data, depending on the inverter and MPPT efficiency at low irradiance, low voltage and partial shading. While the trend in the simulated voltage losses looks similar to what is seen for the measured data in Fig. 2, the losses in current recovers more gradually in Fig. 2 than what is seen in Fig. 4.

Snow covers with increasing transmittance could explain the gradual recovery of the current and power losses seen in Fig. 2. Fig. 5 shows the simulated electrical losses for fully covered modules as a function of snow transmittance. While the current loss is linearly dependent on the transmittance, the losses in voltage are almost recovered as soon as the cells are irradiated.

Fig. 6 gives an example of the combined impact of snow transmittance and coverage, showing how the electrical losses vary with snow transmittance when half of the module is covered. For modules in portrait orientation, the current is still linearly dependent on the transmittance, but in voltage a gain is observed because 50% of the cells are fully irradiated. For the modules in landscape orientation, it is seen that at low transmittance, the shaded module substrings are bypassed giving zero loss in current and 66% loss in voltage. When the transmittance increases and the current loss in the snow-covered module substrings are reduced, the bypass diodes are no longer active resulting in loss in current and zero voltage loss.

While the simulations might explain the trends seen in Fig. 2, they do not explain the variation in losses between different system units. This can, however, be explained by nonuniformity of the snow cover on the system. It is observed that during the process where the snow clears of the modules, there can be variation in both snow coverage and thickness. The total losses are therefore also influenced by the distribution of shading and the configuration of series and parallel connections in the system, as this will affect the maximum power points of the different subarrays.

The impact of both the snow coverage and transmittance on the losses, illustrated in Figs. 4–6, together with the potential nonuniformity of these parameters, explain the trends and the large variations in measured electrical losses during melting shown in Fig. 2. This shows that the assumption of an opaque snow cover in all situations, as is often done in snow loss modeling, is a simplification.

3.1.3. Snow transmittance measurements

To investigate if the transmittance of the snow cover can be high enough to explain the field data observations shown in Fig. 2 as suggested in Section 3.1.2, the transmittance of the snow cover at different thicknesses was measured at the test site. As shown in Fig. 7 and discussed in (Andenæs et al., 2018; Perovich, 2007; Skomedal, 2017), at snow depths less than about 2 cm, transmittance of more than 10%

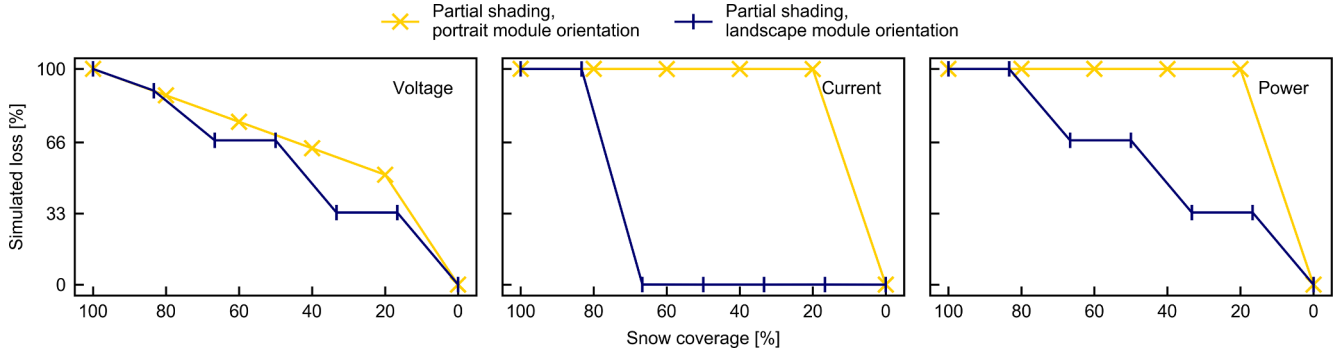

Fig. 4. Simulated losses in voltage, current and power at irradiance of 450 W/m^2 for varying snow coverage with zero transmittance, shown for modules installed in both portrait and landscape orientation.

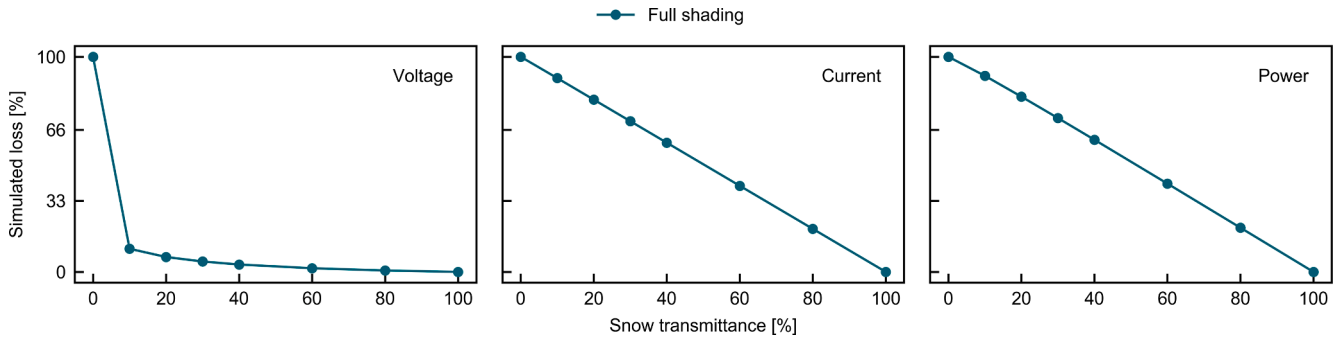

Fig. 5. Simulated losses in voltage, current and power at irradiance of 450 W/m^2 for a full snow cover with varying transmittance.

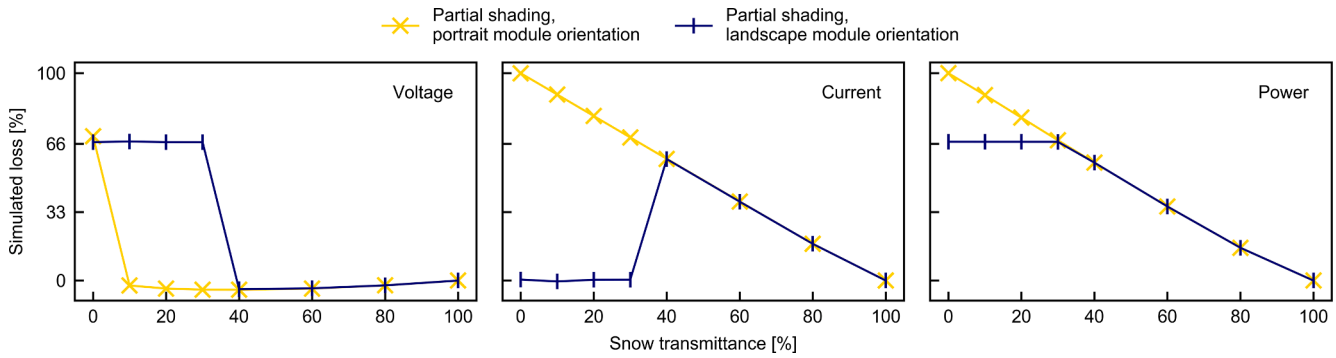

Fig. 6. Simulated losses in voltage, current and power at irradiance of 450 W/m^2 for 50% snow cover with varying transmittance, shown for modules installed in both portrait and landscape orientations.

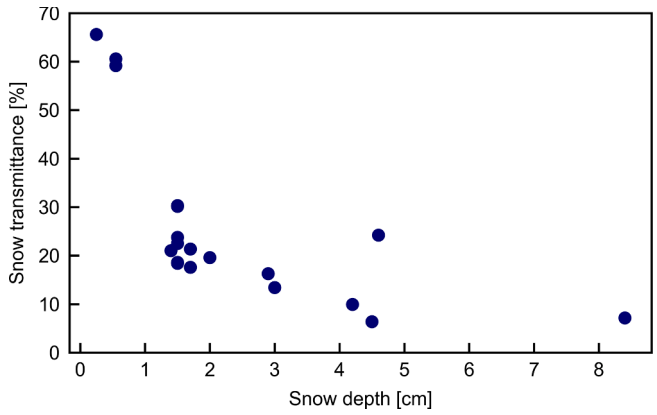

Fig. 7. Measured transmittance of the snow cover on a full size test module glass as a function of snow depth.

might occur. The optical properties of snow is depending on type of snow (Andenæs et al., 2018), so some variations will be expected, but combined with high irradiance, generation of voltage and current is possible at thin snow covers. This is also observed in the electrical measurements of the modules. In situations where the measured snow cover transmittance and irradiance are high, normal voltage values and high current losses are measured. Typically, this is seen in the voltage losses, which for days with snow cover can be very high in the morning and afternoon, and down to zero in the middle of the day when the irradiance is high.

3.1.4. *Snow signature overview*

To summarize the results discussed in Sections 3.1.1–3.1.3, an overview of the impact of different types of snow cover on measured system variables and the overall PV plant behavior, is given in Table 1.

A full opaque snow cover leads to 100% loss in all the electrical parameters. This could be interpreted as an inverter breakdown. To separate the two cases, development in additional parameters such as snow depth and module temperature should be utilized.

When the snow cover is semitransparent and/or partial the situation is more complex, a wider range of outcomes are possible, and larger

Table 1
Overview of different PV parameters for a c-Si monofacial system, and how they are affected by different types of snow covers (full or partial, opaque or semi-transparent) for modules in portrait and landscape orientation.

	Full, opaque	Full, semitransparent	Partial, opaque		Partial, semitransparent	
			Portrait	*Landscape*	*Portrait*	*Landscape*
Module temperature	<< Normal operating temperature		Typically < Normal operating temperature			
DC current	0	Low*	0	Normal	Low	Low-normal*
DC voltage	0	Normal	Low	Low-medium*	High	Low-normal*
Power	0	Low*	0	Low-medium*	Low	Low-medium*
PV plant	No production	All inverters have low/0* power	Many or all of the inverters have low power. There may be large variations in power, current, voltage, and module temperatures.			

* Depending on snow coverage and/or transmittance.

variation within the PV plant is seen. The response in current, voltage and module temperature will depend on both transmittance, size and nonuniformity of the snow coverage, and also on module orientation for crystalline silicon modules. The voltage will be recovered as soon as the cells in the modules are irradiated, either because of clearing of the snow cover or increased transmittance. The maximum current in each module substring will be limited by the least irradiated cell. If partial snow covers lead to variations in irradiance for different module substrings, the bypass diodes in the modules can activate. Because of this, voltage losses during snow covers are characteristic for systems where the modules are installed in landscape orientation, and the typical snow shading is in parallel to the module substrings. No loss in voltage would require snow covers with both high uniformity and high transmittance, which is possible, but not very common. How many bypass diodes that are active depends on the transmittance and uniformity of the snow cover. For module substrings with snow covers with high transmittance, active bypass diodes and voltage losses can lead to larger power losses than when the diodes are not active, as illustrated in Fig. 6. If one shaded module substring is not bypassed, this gives a loss in current in addition to the voltage loss, as observed for the commercial system in Fig. 2.

3.2. Snow loss model evaluation

The snow loss models described in Section 2.3 were evaluated for the commercial system (landscape orientation). The loss was measured for all the inverters in the system to capture eventual variations in snow losses for identical system configurations. Due to its small size and severe system shading for some parts of the winter, the test system was not found suitable for model evaluation.

3.2.1. Evaluation of empirical snow loss models

The models built on empirical correlations between ambient conditions and losses, failed to estimate snow losses satisfactorily, particularly when there were differences in ambient conditions between the tested dataset and the dataset the model was based on. For the model suggested by Andrews and Pearce (2012), the R^2 of the relationship between the power loss and the suggested explanatory parameters was 0.24, showing a low correlation. The snow data in this model is limited to snow fall data from the two previous days. For the dataset in this study, however, snow covers can in some cases last longer than a month. For the simple model for yearly relative losses suggested by Powers et al. (2010), the modeled losses were 2.3–5% compared to measured losses of 2.2–11.2%. For most years, the difference between measured and modeled losses was below 1 percentage point, but for the year with largest losses, the difference was 6.2 percentage points. Different ambient conditions might also here be influential: in Truckee, California, where the model is developed, the difference in total irradiation from summer to winter is lower than for the data in this study because of the difference in latitude. For the Norwegian location, the irradiance changes a lot through the year, and the time of the snow cover also influences the total losses, as snow cover in the middle of the winter will have less impact on the annual losses than a springtime snow cover. The second model developed by Townsend and Powers (2011), had a mean absolute error in the estimation of relative monthly snow losses of 23%.

3.2.2. The Marion snow loss model

The empirical models can be used to give rough estimates of the losses, but for models based on a few datasets, it appears to be difficult to capture all aspects of snow covers and resulting PV losses and develop accurate and transferable models. Modeling different aspects of snow covers and losses separately and aim for modeling of absolute losses, like in the Marion model, was shown to be a more robust and flexible approach, yielding more accurate loss estimations. The threshold defined in Eq. (1). to identify sliding events caused by snow melting, correlated well with melting events found in the snow data. Most melting events, and all large melting events, could be predicted by the conditions defined in Eq. (1). The default sliding coefficient in pvlib (0.20), estimated for roof mounted systems, was however observed to be too high. This coefficient is expected to depend on different system and module designs, because technical aspects can either promote or obstruct snow sliding (Burnham et al., 2020). Frameless modules (Riley et al., 2019), empty space below modules (Heidari et al., 2015), and heating on the rear side of the module (Ross, 1995) (e.g. from reflected irradiance – in particular for bifacial modules (Burnham et al., 2019), or the building if roof mounted) will promote sliding, for instance. In the studied case, where the modules are installed on a flat, well-insulated roof, and there is no empty space where sliding snow can accumulate below the modules, high roof interference and a low sliding coefficient is expected (Heidari et al., 2015). Generally, when the snow depth is increasing, the empty space below the modules will decrease, giving increased ground/roof interference. In this case, because the modules are not elevated, how much the snow can slide down the module surface will also decrease with increasing snow depth. The top of the modules is approximately 30 cm above the rooftop. With snow depths above 30 cm, the system will be fully submerged in snow and there will be no sliding. Snow depths above 30 cm are rare for the tested system, as shown in Fig. 10, but the observed snow depths do often lead to situations where the system is partly submerged in snow, reducing the possibility for snow sliding. Melting is therefore most likely an important snow clearing mechanism in the tested system, a process that typically is slower than sliding for thick snow layers. Fig. 8 shows for different *sc* values, for periods with snow depth > 3 cm, how measured snow loss correlate with modeled snow cover, and the correlation between measured and modeled daily snow loss. Fig. 8 a) shows how a larger fraction of the timestamps with measured snow loss correlate with timestamps with modeled snow cover, both for high and lower measured snow loss, when using a lower sliding coefficient. As shown in Fig. 8 b), reducing the sliding coefficient gives a better fit between measured and modeled daily losses. Here, because the Marion model assumes zero production from partly covered module substrings and a uniform snow cover, the modeled loss is stepwise, and the only possible outcomes are 0, 33%, 66% or 100% loss. As shown in Fig. 2, the measured power loss has a wider range of outcomes. Some of the variations in the measured losses, can also be caused by the high relative errors in the modeled daily expected power for parts of the winter periods.

The data show that for thin snow covers, however, snow clearing happened significantly faster. There is more room for snow to slide down the module surface, and thin snow covers are also more likely to melt directly on the module, a process that for thin snow covers is faster than sliding (Andrews et al., 2013; Pawluk et al., 2019). Additionally, as thin snow covers have higher transmittance, heating of the module that can aid the melting is expected (Pawluk et al., 2019). As shown in Fig. 9, when the measured snow depth is low, the sliding coefficient that most consistently models 100 or 66% loss in periods with high losses, and 0 or 33% in periods with low losses, is 0.4, which is higher than what was seen in Fig. 8. For the test system it is also observed that the sliding coefficient seems to be influenced by the snow conditions. In Fig. 9, it is also seen that the modeled losses for thin snow covers shows a poorer fit with measured loss compared to thicker snow covers. Thin snow covers have also previously been shown to introduce noise in loss modeling (Andrews and Pearce, 2012). In addition to the challenge of exact estimation of snow coverage, snow transmittance is, as previously discussed, playing a role for thin snow covers and might challenge the loss estimation.

As shown in Fig. 10, reducing the sliding coefficient to 0.06 compared to the default sliding coefficient in pvlib of 0.20, gave a better fit between measured and modeled losses for most years. The exception is 2017, a year with very low snow depths. Also shown in Fig. 10, introducing separate sliding coefficients (or more general: snow *clearing* coefficients) for snow depths above and below 3 cm yields an even better fit with the total measured losses. With the default *sc* the total modeled absolute snow loss for the five years of data was underestimated by 23%,

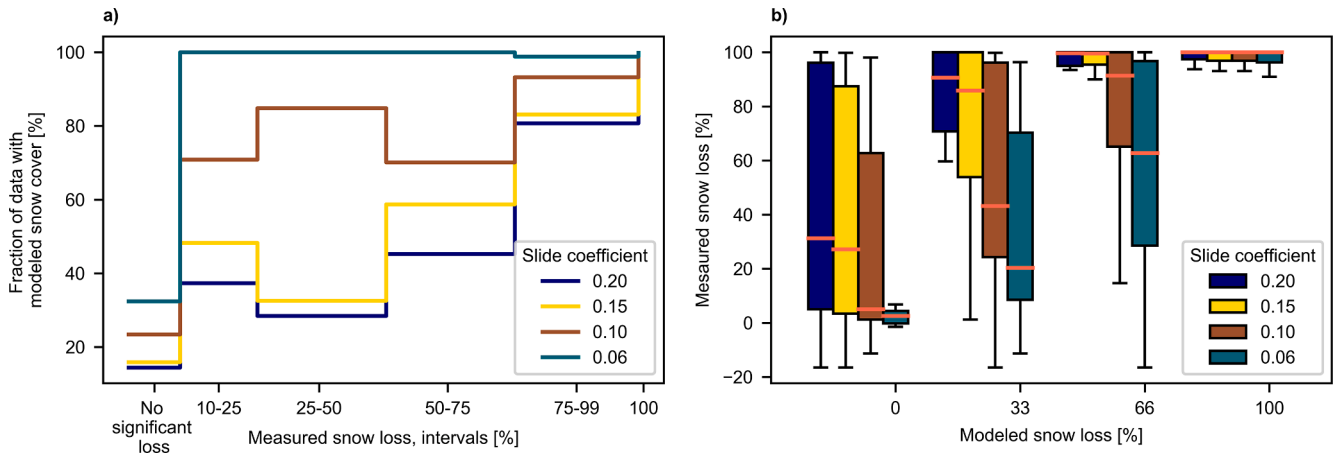

Fig. 8. For periods with snow depths > 3 cm and with four different sliding coefficients used in snow cover/loss modeling, a) the fraction of data for different power loss intervals with modeled snow cover > 0 (due to the uncertainty in the modeling of the expected power, 10% is set as the lower limit of significant snow loss), and b) the variation in daily measured loss at the different modeled loss values (four possible outcomes: 0, 33, 66 and 100%). The boxes extend from the first to the third quartile values of the data, with a line on the median. The whiskers extend to the maximum or minimum value within 1.5 times the interquartile range, and outliers are not included.

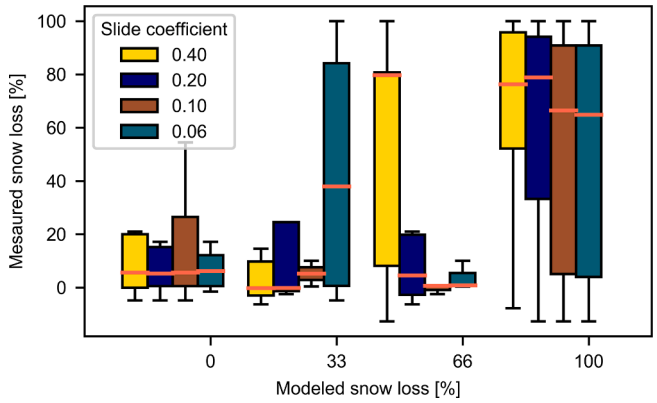

Fig. 9. For periods with snow depths < 3 cm and with four different sliding coefficients used in snow cover/loss modeling, the variation in daily measured loss at the different modeled loss values (four possible outcomes: 0, 33, 66 and 100%). The boxes extend from the first to the third quartile values of the data, with a line on the median. The whiskers extend to the maximum or minimum value within 1.5 times the interquartile range and outliers are not included.

with the reduced *sc* (0.06) the losses were overestimated by 11%, and with the snow depth dependent *sc* the model overestimated by 3%, yielding a significant improvement to the model. Relative to the mean yearly energy generation in the analysis period, the differences in measured and modeled losses when using the model with snow depth dependent *sc*, was between −0.8 and 0.3 percentage points.

It would still be expected that snow loss modeling is still not exact on high time resolutions even with improved sliding coefficients, both due to challenges with estimating the snow coverage, the transmittance and non-uniformity of the snow coverage, and the difficulty of accurately quantifying the effect the snow has on the PV production. It can, however, be used to assess the probability of snow cover on the modules and give reasonable snow loss estimates for yield estimations which are typically aggregated to lower time resolutions.

3.3. Snow detection

The observed snow signatures in the data and the improved snow model are promising starting points for building snow detection algorithms for monitoring purposes, failure diagnosis and performance loss analysis. While snow loss modeling has too low accuracy on high time

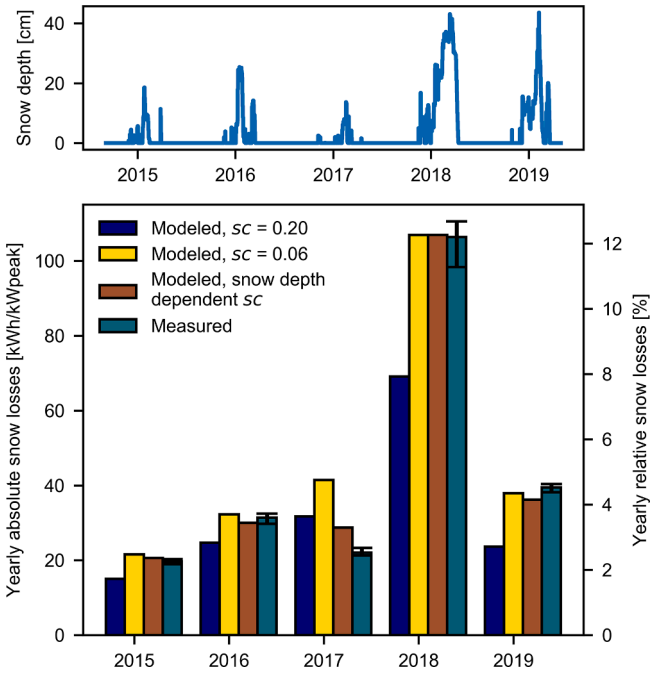

Fig. 10. Measured (plant median) and modeled yearly absolute and relative snow losses. The relative losses are calculated based on the mean yearly expected energy generation in the analysis period. The error bar shows the range of the measured losses in the PV plant. The snow losses are modeled in pvlib with default sliding coefficient (0.20), reduced sliding coefficient (0.06) and a snow depth dependent coefficient: 0.4 for snow depth < 3 cm, and 0.06 for snow depths > 3 cm. The corresponding snow depth measurements are also shown.

resolutions to directly model losses in monitoring, the improved snow cover model suggested in Section 3.2 can be used to indicate the possibility of snow-covered modules, as shown in Fig. 8 a). For the tested commercial system, the loss in voltage is the signature that in most cases is connected to snow loss, as discussed in Section 3.1.4. Fig. 11 shows, for different power loss intervals, how large share of the data that would be labeled as snow, given a snow detection criterion of: 1) voltage loss between 10% and 100%, 2) modeled snow cover larger than 0, 3) either criterion 1 or 2. The data has 5-minute resolution and is taken from

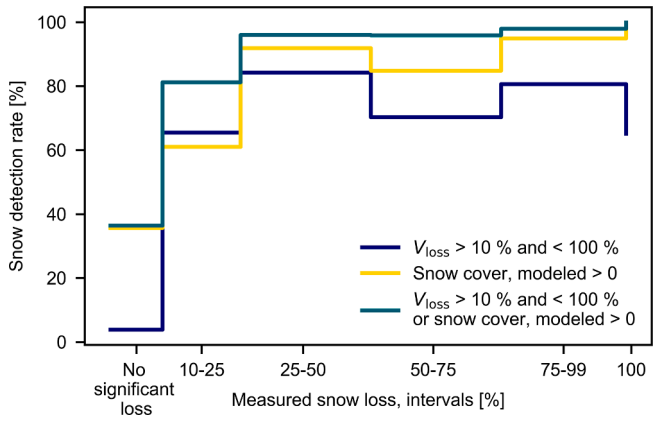

Fig. 11. Snow detection rate for different intervals of measured snow loss for the following criteria: 1) voltage loss between 10% and 100%, 2) modeled snow cover greater than zero, and 3) either 1 or 2. Only data points from periods with snow on the ground and irradiance above 50 W/m^2 are considered. Due to the uncertainty in the modeling of the expected power, 10% is set as the lower limit of significant snow loss.

periods with irradiance above 50 W/m^2 and snow on the ground. For the third criterion, 97% of the snow losses above 10% is labeled as snow. The detection rate is higher at high snow loss. At full snow covers giving 100% loss, the detection rate is 100%. In periods with a measured power loss smaller than 10%, i.e. no significant snow loss, 38% of the data points are labeled as snow, which we interpret as false positives. These false positives are mostly related to the uncertainty in the snow loss modeling for thin snow covers and during melting, causing the model to indicate snow cover in periods where the snow has been cleared. A consequence of false positives in snow detection could be that actual system faults are falsely labeled as snow losses. Snow loss modeling is consequently best used to indicate the probability of snow cover.

To improve snow detection, more of the snow signatures described in Section 3.1 could be included. The module temperature measurements and the duration and evolution of the snow signatures could e.g. be taken into account. Snow losses, especially during snow melting, can change significantly from day to day and within a day, in a different way than typical system faults. The results suggest that due to the high rate of the data with losses that correctly are identified as snow, the snow detection method will improve fault detection and diagnosis as well as loss analysis, and that further improvements could be achieved by including more of the identified snow signatures and by using snow loss modeling to indicate probability of snow cover.

4. Conclusions

In this paper we describe the effect of different types of snow cover on PV energy generation, and snow related signatures in PV monitoring data are identified. In addition to snow coverage and system configuration, transmittance and nonuniformity of the snow cover influence the total snow losses, increasing the complexity in snow loss modeling. Existing snow loss models are evaluated. Three of the models are purely empirical, and power loss is directly estimated based on system and weather data. In the Marion model empirical correlations are used to model different effects causing natural snow clearing, and snow coverage and the resulting loss are modeled separately. We find that the purely empirical models are less general and flexible than the Marion model.

For the evaluated system with low tilt modules on a flat roof, the natural snow clearing rate is observed to be much faster for thin snow covers (<~2–3 cm) than for thicker snow covers. This difference in the snow clearing process between thin and thick snow covers is assumed to be especially large for the evaluated system. This is because there is little available space where the snow can slide away, leading to slow snow clearing for thick snow covers. The evaluated system design is, despite this, very common in the Nordic countries because it gives increased roof coverage and more even energy generation throughout the year. By including the effect of snow depth dependent snow clearing in the Marion model, we achieve reduced uncertainty in the modeled snow losses, allowing more accurate energy yield assessment for new PV systems. We also find that the identified snow data signatures and the improved Marion snow model can be used to detect and separate snow losses from other phenomena that affects PV production, such as faults. This is important for the development of PV in cold climate areas that are prone to snow.

We discuss how different system designs can promote or obstruct snow clearing, and we find that for the tested system the snow clearing rate is lower than for the systems the snow sliding/clearing coefficients in the Marion model is based on. Future work should therefore include further validation of the snow clearing coefficients for different system designs. Additionally, as snow is a complex weather phenomenon, validation of the improved model and the snow detection for larger datasets and different environments is necessary. The aspect of the evolution of the snow data signatures with time should also be further investigated to improve snow detection.

Declaration of Competing Interest

The authors declare that they have no known competing financial interests or personal relationships that could have appeared to influence the work reported in this paper.

Acknowledgments

The authors acknowledge funding from the Innovation project number 803801 (Autonomous monitoring, control and protection of renewable energy infrastructure) and RCN 282357 - Smart styring av næringsbygg med lokal strømproduksjon.

References

Aarseth, B.B., Øgaard, M.B., Zhu, J., Strömberg, T., Tsanakas, J.A., Selj, J.H., Marstein, E. S., 2018. Mitigating snow on rooftop PV systems for higher energy yield and safer roofs. In: Proceedings of the 35th European Photovoltaic Solar Energy Conference and Exhibition, pp. 1630–1635. https://doi.org/10.4229/35thEUPVSEC2018-6CO.3.5.

Andenæs, E., Jelle, B.P., Ramlo, K., Kolås, T., Selj, J., Foss, S.E., 2018. The influence of snow and ice coverage on the energy generation from photovoltaic solar cells. Sol. Energy 159, 318–328. https://doi.org/10.1016/j.solener.2017.10.078.

Andrews, R.W., Pearce, J.M., 2012. Prediction of energy effects on photovoltaic systems due to snowfall events. In: 2012 38th IEEE Photovoltaic Specialists Conference. IEEE, pp. 3386–3391. https://doi.org/10.1109/PVSC.2012.6318297.

Andrews, R.W., Pollard, A., Pearce, J.M., 2013. The effects of snowfall on solar photovoltaic performance. Sol. Energy 92, 84–97. https://doi.org/10.1016/j.solener.2013.02.014.

Bashir, N., Irwin, D., Shenoy, P., 2020. DeepSnow: Modeling the impact of snow on solar generation. In: Proceedings of the 7th ACM International Conference on Systems for Energy-Efficient Buildings, Cities, and Transportation. pp. 11–20. https://doi.org/10.1145/3408308.3427620.

Becker, G., Schiebelsberger, B., Weber, W., Vodermayer, C., Zehner, M., Kummerle, G., 2006. An approach to the impact of snow on the yield of grid connected PV systems. Proceedings of the 21st European Photovoltaic Solar Energy Conference and Exhibition.

Bosman, L.B., Darling, S.B., 2018. Performance modeling and valuation of snow-covered PV systems: examination of a simplified approach to decrease forecasting error. Environ. Sci. Pollut. Res. 25, 15484–15491. https://doi.org/10.1007/s11356-018-1748-1.

Burnham, L., Riley, D., Braid, J., 2020. Design considerations for photovoltaic systems deployed in snowy climates. In: Proceedings of the 37th European Photovoltaic Solar Energy Conference and Exhibition, pp. 1626–1631.

Burnham, L., Riley, D., Walker, B., Pearce, J.M., 2019. Performance of bifacial photovoltaic modules on a dual-axis tracker in a high-latitude, high-albedo environment. In: 2019 46th IEEE Photovoltaic Specialists Conference. IEEE, pp. 1320–1327. https://doi.org/10.1109/PVSC40753.2019.8980964.

Dobos, A.P., 2012. An improved coefficient calculator for the California energy commission 6 parameter photovoltaic module model. J. Sol. Energy Eng. 134 https://doi.org/10.1115/1.4005759.

FME Susoltech, 2020. Interactive map of monitored PV installations in Norway, IFE test site, Kjeller. [WWW Document]. URL https://susoltech.no/solar-panel-map/ (accessed 12.22.20).
Gilman, P., Dobos, A., DiOrio, N., Freeman, J., Janzou, S., Ryberg, D., 2018. SAM photovoltaic model technical reference update, No. NREL/TP-6A20-67399. Golden.
Hashemi, B., Cretu, A.M., Taheri, S., 2020. Snow loss prediction for photovoltaic farms using computational intelligence techniques. IEEE J. Photovoltaics 10, 1044–1052. https://doi.org/10.1109/JPHOTOV.2020.2987158.
Heidari, N., Gwamuri, J., Townsend, T., Pearce, J.M., 2015. Impact of snow and ground interference on photovoltaic electric system performance. IEEE J. Photovoltaics 5, 1680–1685. https://doi.org/10.1109/JPHOTOV.2015.2466448.
Holmgren, W.F., Hansen, C.W., Mikofski, M.A., 2018. pvlib python: a python package for modeling solar energy systems. J. Open Source Softw. 3, 884. https://doi.org/10.21105/joss.00884.
IEA, 2020. PVPS Trends in photovoltaic applications 2020.
Jäger-Waldau, A., 2020. Snapshot of photovoltaics—February 2020. Energies 13.
King, D.L., Kratochvil, J.A., Boyson, W.E., 2004. Photovoltaic array performance model, No. SAND2004-3535. Albuquerque. https://doi.org/10.2172/919131.
Lorenz, E., Betcke, J., Drews, A., de Keizer, A.C., Stettler, S., Scheider, M., Bofinger, S., Beyer, H.G., Heydenreich, W., Wiemken, E., van Sark, W., Toggweiler, P., Heilscher, G., Heinemann, D., 2007. Intelligent performance check of PV system operation based on satellite data (PVSAT-2), final technical report.
Lorenz, E., Heinemann, D., Kurz, C., 2011. Local and regional photovoltaic power prediction for large scale grid integration: Assessment of a new algorithm for snow detection. Prog. Photovoltaics Res. Appl. 20, 760–769.
Marion, B., Schaefer, R., Caine, H., Sanchez, G., 2013. Measured and modeled photovoltaic system energy losses from snow for Colorado and Wisconsin locations. Sol. Energy 97, 112–121. https://doi.org/10.1016/j.solener.2013.07.029.
Norsk Klimaservicesenter, 2020. Observasjoner og værstatistikk [WWW Document]. URL https://seklima.met.no/observations/ (accessed 12.22.20).
NREL, 2020. PySAM.
NVE, 2019. seNorge [WWW Document]. URL www.senorge.no (accessed 9.1.19).
Øgaard, M.B., Haug, H., Selj, J., 2018. Methods for quality control of monitoring data from commercial PV systems. In: Proceedings of the 35th European Photovoltaic Solar Energy Conference and Exhibition, pp. 2083–2088. https://doi.org/10.4229/35thEUPVSEC20182018-6DV.1.53.
Øgaard, M.B., Riise, H.N., Haug, H., Sartori, S., Selj, J.H., 2020. Photovoltaic system monitoring for high latitude locations. Sol. Energy 207. https://doi.org/10.1016/j.solener.2020.07.043.
Pawluk, R.E., Chen, Y., She, Y., 2019. Photovoltaic electricity generation loss due to snow – A literature review on influence factors, estimation, and mitigation. Renew. Sustain. Energy Rev. 107, 171–182. https://doi.org/10.1016/j.rser.2018.12.031.
Perovich, D.K., 2007. Light reflection and transmission by a temperate snow cover. J. Glaciol. 53, 201–210. https://doi.org/10.3189/172756507782202919.
Powers, L., Newmiller, J., Townsend, T., 2010. Measuring and modeling the effect of snow on photovoltaic system performance. In: 2010 35th IEEE Photovoltaic Specialists Conference. IEEE, pp. 973–978. https://doi.org/10.1109/PVSC.2010.5614572.
PVGIS, 2020. Data sources and calculation methods [WWW Document]. URL https://ec.europa.eu/jrc/en/PVGIS/docs/methods (accessed 12.22.20).
PVsyst, 2020. Soiling loss [WWW Document]. URL https://www.pvsyst.com/help/index.html (accessed 12.22.20).
Riley, D., Burnham, L., Walker, B., Pearce, J.M., 2019. Differences in snow shedding in photovoltaic systems with framed and frameless modules. In: 2019 46th IEEE Photovoltaic Specialists Conference. IEEE, pp. 558–561. https://doi.org/10.1109/PVSC40753.2019.8981389.
Ross, M., 1995. Snow and ice accumulation on photovoltaic arrays: An assessment of the TN conseil passive melting technology, Division Report EDRL 95-68 (TR). Varennes.
Ryberg, D., Freeman, J., 2017. Integration, validation, and application of a PV snow coverage model in SAM, NREL/TP-6A20-68705. Golden.
Schill, C., Brachmann, S., Koehl, M., 2015. Impact of soiling on IV-curves and efficiency of PV-modules. Sol. Energy 112, 259–262. https://doi.org/10.1016/j.solener.2014.12.003.
Skomedal, Å., 2017. The transmittance of light through snow; an initial study for solar energy systems. https://doi.org/10.13140/RG.2.2.10539.54568.
Solargis, 2016. Solargis pvPlanner User Manual.
Souka, A.F., Safwat, H.H., 1966. Determination of the optimum orientations for the double exposure flat-plate collector and its reflections. Sol. Energy 10, 170–174.
Stein, J.S., Farnung, B., 2017. PV performance modeling methods and practices, Report IEA-PVPS T13-06:201.
Teubner, J., Buerhop, C., Pickel, T., Hauch, J., Camus, C., Brabec, C.J., 2019. Quantitative assessment of the power loss of silicon PV modules by IR thermography and its dependence on data-filtering criteria. Prog. Photovoltaics Res. Appl. 27, 856–868. https://doi.org/10.1002/pip.3175.
Townsend, T., Powers, L., 2011. Photovoltaics and snow: An update from two winters of measurements in the Sierra. In: 2011 37th IEEE Photovoltaic Specialists Conference. IEEE, pp. 3231–3236. https://doi.org/10.1109/PVSC.2011.6186627.
Tsanakas, J.A., Ha, L., Buerhop, C., 2016. Faults and infrared thermographic diagnosis in operating c-Si photovoltaic modules: A review of research and future challenges. Renew. Sustain. Energy Rev. 62, 695–709. https://doi.org/10.1016/j.rser.2016.04.079.
van Noord, M., Berglund, T., Murphy, M., 2017. Snöpåverkan på solelproduktion om snöförluster på takanläggningar i Norra Sverige., Rapport 2017:382.
Wirth, G., Schroedter-Homscheidt, M., Zehner, M., Becker, G., 2010. Satellite-based snow identification and its impact on monitoring photovoltaic systems. Sol. Energy 84, 215–226. https://doi.org/10.1016/j.solener.2009.10.023.